ARTICLE

BIOTECHNOLOGY and BIOENGINEERING

Label-Free Identification of Bacterial Microcolonies Via Elastic Scattering

Euiwon Bae,[1] Nan Bai,[1] Amornrat Aroonnual,[2] Arun K. Bhunia,[2] E. Daniel Hirleman[1]

[1]School of Mechanical Engineering, Purdue University, West Lafayette, Indiana 47906; telephone: 765-494-4762; fax: 765-494-0539; e-mail: ebae@purdue.edu

[2]Molecular Food Microbiology Laboratory, Department of Food Science, Purdue University, West Lafayette, Indiana 47906

Received 18 August 2010; revision received 24 September 2010; accepted 12 October 2010

Published online 28 October 2010 in Wiley Online Library (wileyonlinelibrary.com). DOI 10.1002/bit.22980

ABSTRACT: Label-free microcolony identification via elastic light scattering was investigated for three different genera: *Salmonella enterica* serovar Montevideo, *Listeria monocytogenes* F4244, and *Escherichia coli* DH5α. Microcolonies were defined as bacterial colonies in their late-lag phase to early-exponential phase with the diameter range of 100–200 μm. To link biophysical characteristics with corresponding scattering patterns, a phase contrast microscope and a confocal displacement meter were used to measure the colony diameter and its 3D height profile. The results indicated that the growth characteristics of microcolonies were encoded in their morphologies which correlated to the characteristic diffraction patterns. Proposed methodology was able to classify three genera based on comprehensive phenotypic map which incorporated growth speed, ring count, and colony diameter. While the proposed method illustrated the possibility of discriminating microcolonies in their early growth stage, more thorough biophysical understanding is needed to expand the technology to other species.

Biotechnol. Bioeng. 2011;108: 637–644.

© 2010 Wiley Periodicals, Inc.

KEYWORDS: microcolony; light scattering; Identification; colony morphology

Introduction

A series of recent outbreaks demands more rapid, reliable, and sensitive analytical methods in monitoring pathogenic microorganism such as *Salmonella* (Heaton and Jones, 2008; Van Duynhoven et al., 2009), *Escherichia coli* (Heaton and Jones, 2008; King et al., 2009), and *Listeria* (Cumming et al., 2009; Shetty et al., 2009; Swaminathan and Gerner-Smidt, 2007) to name a few. Since contaminations could happen from harvest to distributions, it is critical to provide accurate and rapid identification and classification of pathogens to monitor and react to any possible outbreak situations. A number of conventional methodologies used in bacterial identification include morphological observations (Stecchini et al., 2000; Tetz et al., 1993), serological tests (Gehring et al., 2006), proteomics (Cash, 2009; Cash and Hecker, 2003), and genomics (Jaradat et al., 2002). Among these, morphological methods sought phenotypic characteristics of a bacterial species to differentiate from other species. Traditionally, these methods relied on observable characteristics of the individual colony, such as: Color, shape, and growth rate. Since Wyatt (Wyatt, 1969), light scattering has been widely used to provide fast, accurate, and non-disruptive interrogation of biological samples (Bronk et al., 1992, 2001; Jones et al., 1998; Kottmeier et al., 2009; Samorski et al., 2005). While these examples mostly dealt with cells in liquid state, our group introduced a new concept of using laser to interrogate the bacterial colonies to generate unique scattering patterns which worked as an individual "fingerprint" for each bacterial kind (Bae et al., 2007, 2009, 2010). This technology provided label-free, fast, and reliable identification of bacterial species via comparing the scattering patterns with the previously recorded image database. Even though the proposed system provided faster identification than the conventional plating method, the throughput was limited by the incubation time of the individual colony to reach a certain diameter. For example, *Listeria* required 24–30 h while *E. coli* and *Salmonella* needed 12 h to satisfy the diameter criterion (Bae et al., 2008; Banada et al., 2009). This growth time imposes a bottle-neck to the first responders of the outbreak situation and government/corporate laboratories operating on 8 h shift could not obtain the identification within one work-shift.

Recently, a new research field has been highlighted for providing identification in the early stage of bacterial growth. If we define the traditional diameter regime as a

Amornrat Aroonnual's present address is Department of Tropical Nutrition and Food Science, Faculty of Tropical Medicine, Mahidol University 420/6 Ratchawithi Road, Ratchathewi, Bangkok 10400. Thailand.

E. Daniel Hirleman's present address is School of Engineering, University of California Merced, Merced, CA 95343 USA.

Correspondence to: Euiwon Bae

Contract grant sponsor: US Department of Agriculture

Contract grant sponsor: Center for Food Safety and Engineering at Purdue University

© 2010 Wiley Periodicals, Inc.

macrocolony, the new area of interest shall be called microcolonies when the bacterial colonies are within 100–200 μm in diameter. Colonies at this stage possess various biochemical and biophysical differences compared to the macrocolonies. First, in the viewpoint of the conventional Sigmoidal growth curve (lag-exponential-stationary phase), we were interested in the end of the lag phase or the start of the exponential phase. Second, bacteria colonies were in their earlier growth stage and rapidly growing, so a tight control of the measurement window was required compared to the bacterial colonies at the stationary phase. Third, as the colony diameter became smaller, the instrument had to accommodate the change in the colony diameter to deliver effective and distinctive scattering patterns. Raman and FTIR (Choo-Smith et al., 2001; Goodwin et al., 2006) were applied to investigate the homogeneity and heterogeneity of one species as the colony grew. The result indicated that microcolonies were quite homogeneous and thus, their spectra could be used as references to construct a database across different species, while macrocolonies showed spatial heterogeneities. Some researchers provided an automatic enumeration system for the microcolonies of approximately 50 μm (Wang et al., 2007). However, to capture the images of microcolonies, they had to stain the bacteria with SYBR Green II. Other researchers have used similar techniques to count the viable bacteria within contaminated platelet concentrates using both fluorescent staining and morphological characteristics (Motoyama et al., 2008). These techniques were also applied for identifying beer-spoilage lactic acid bacteria within microcolony size regime (Asano et al., 2009). These image based detection systems, in order to detect and differentiate the bacteria at their early stages, commonly needed fluorescent dyes or staining agents to provide for a sufficient contrast from the surrounding environment and to achieve specific recognition. In this paper, the microcolony identification system was presented as a label-free means to interrogate the bacterial colonies within microcolony regime. Here, the elastic scattering technique was used to generate unique scattering patterns among different genera which were correlated with the independent colony morphology measurements. Three different genera, *Salmonella* Montevideo, *Escherichia coli* DH5α, and *Listeria monocytogenes* F4244 were investigated to correlate their microcolony morphology and the scattering patterns.

Materials and Methods

Sample Preparation

The *S.*Montevideo, *L. monocytogenes* F4244, and *E. coli* DH5α cultures were selected to be inoculated in brain heart infusion (BHI) broth and incubated at 37°C overnight. The culture was then diluted (10-fold dilution to 10^{-6}) in phosphate buffer saline. The 100 μL of appropriated concentration was thoroughly spread on BHI agar and cultivated at 37°C in the incubator. To accommodate the different growth rate to reach the target microcolony size, incubation times were controlled differently. Six plates were prepared for each species. After the first six and a half hour incubation for *E. coli* DH5α and *S.*Montevideo and 10 h incubating for *L. monocytogenes*, one plate per species was taken out every half an hour with five samples selected from each plate to be measured by a phase contrast microscope. This process was repeated four times to give a total number of twenty samples at each time interval. It took approximately 7 and 9 h for *S.*Montevideo and *E. coli* DH5α to grow into our targeting diameter range (100–200 μm). Since *L. monocytogenes* is slowly growing organism, it took 12 h to reach the designated diameter range.

System Description

In the microcolony experiment via forward scattering, it was critical to control the beam diameter comparable to that of the microcolony (Siegman, 1986). When the colony diameter was larger than the laser beam there was an un-interrogated area that could possibly provide cirtical phenotypic information about the colony, while in the opposite case, the incident laser signal dominated the forward scattering signature and saturated the detector. To avoid both situations, we designed the scatterometer with a biconvex lens which rendered the beam waist of 100–200 μm within the Raleigh range (Siegman, 1986) and the estimated depth of field was sufficiently larger than the colony thickness (~10–20 μm). The optical setup consisted of a diode laser with wavelength of 635 nm (coherent 0221-698-01 REV B, CA), with the output beam diameter of 1 mm with a divergence of 1.3 mrad. A single bi-convex lens (BK7 H32-717, Edmund Optics, Barrington, NJ) with a focal length of 150 mm was used to reduce the size of the laser beam spot. The motion control part consisted of *X*–*Y* motorized stages to move the petri dish in the *X*–*Y* plane to align the laser with the center of each selected bacterial colony and a linear translation stage (Edmund Optics) along the vertical *Z*-axis to adapt the laser beam size to the bacterial colony size within the Raleigh range. The *X*–*Y* stages were translated by two linear motors (850G-HS, Newport, Irvine, CA) connected to the multi-axis closed-loop controller (ESP300, Newport) with the specification of a 42 mm maximum stroke and a 0.1 μm minimum step size. A monochromatic IEEE1394 CMOS array (PixeLINK, Ottawa, ON, Canada) with a 1280×1024 resolution and at $6.7 \times 6.7\ \mu m^2$ for each pixel was integrated as the imaging sensor.

Phase Contrast Microscope and Confocal Displacement Meter

The phase contrast microscope (PCM; Leica, McHenry, IL) was used to measure the diameters of the microcolonies and to observe microstructures, such as spokes, dots, and cracks within the colonies. This, however, does not provide any quantitative information about the physical profiles of the bacterial colonies. Therefore, the confocal displacement meter (CDM; Keyence LT9010, NJ) was integrated with the

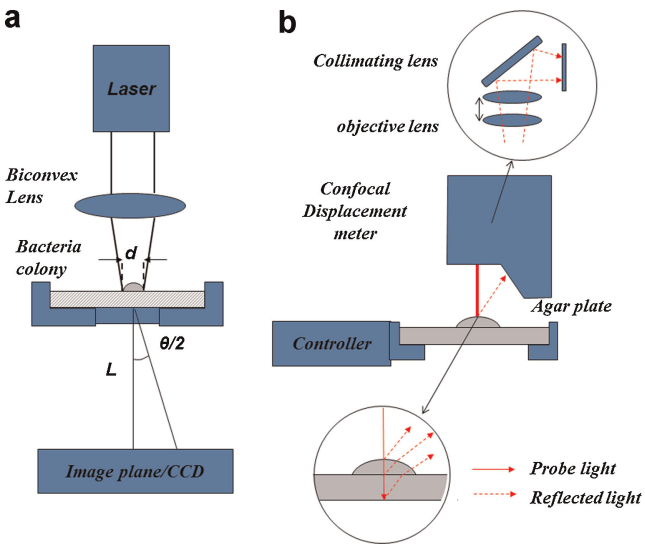

Figure 1. **a**: The schematic diagram of the forward scatterometer for micro-colonies. A biconvex lens with $f = 150$ mm was used to approximately match the incident Gaussian beam diameter with the diameter of the bacterial colony under investigation. **b**: Colony profile measurement via a CDM where incident probe beam was reflected from multiple surfaces. By actively controlling the collimating and objective lens to reject the out-of-focus light, the CDM could obtain accurate profile measurement data from a transparent surface. [Color figure can be seen in the online version of this article, available at wileyonlinelibrary.com.]

X–*Y* motorized stages to obtain the profile of each individual bacterial colony to provide comparisons among the different species (Fig. 1b). Since bacterial colonies were semi-transparent objects, the probing laser was reflected back from multiple surfaces where conventional laser triangulation sensor did not provided reliable results (data not shown). To effectively measure the profile of semi-transparent samples, confocal principle was integrated to actively select the reflected lights from in-focus surface and reject the out-of-focus lights. This instrument implemented a high accuracy surface scanning method by using a 670 nm laser light source with the spot size of 2 μm and the vertical reference distance of 6 mm and a scanning resolution up to 0.01 μm (Keyence-Corporation 2006).

After the diameter measurement by the PCM, the plate was taken to the CDM for profile characterization. The instrument operated in a profile mode with a scanning width of 1100 μm and a scanning interval of 5 μm along the *X* direction. Along the *Y* direction, the stage was translated with a 5 μm resolution and a 200 μm length to capture the complete profile of the colony. It took approximately 15–20 min for a complete measurement on single colony.

Results

Scattering Patterns

Figure 2 displays a series of scattering patterns with varying colony diameters (measured with the PCM) which were recorded after different incubation time for each genus (7, 9, and 12 h for *S.*Montevideo, *E. coli* DH5α, and *L. monocytogenes* F4244). One interesting feature was that the number of rings of scattering patterns increased as the diameter of the colony grew. For example, *S.*Montevideo (124 μm) and *L. monocytogenes* F4244 (134 μm) generated approximately six diffraction rings while *E. coli* DH5α (129 μm) generated only four rings. In addition, fast growing bacteria (*S.*Montevideo and *E. coli* DH5α) displayed irregular shaped ring patterns which arise from rugged colony edges, while *L. monocytogenes* F4244, which grew slower than the other two genera, generated smoother ring patterns.

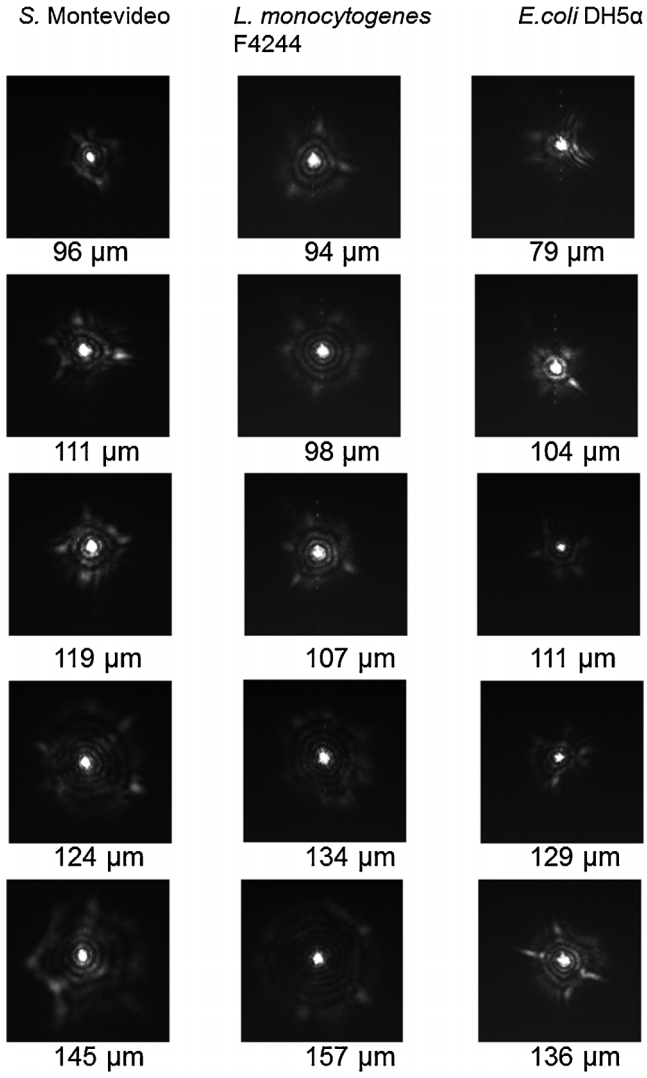

Figure 2. A series of forward scattering patterns of microcolonies for three genera:(left) *S.*Montevideo, (center) *L. moncytogenes* F4244, and (right) *E. coli* DH5α. The diameter ranges from 96 to 145 μm, 94 to 157 μm, and 79 to 136 μm for these three genera, respectively.

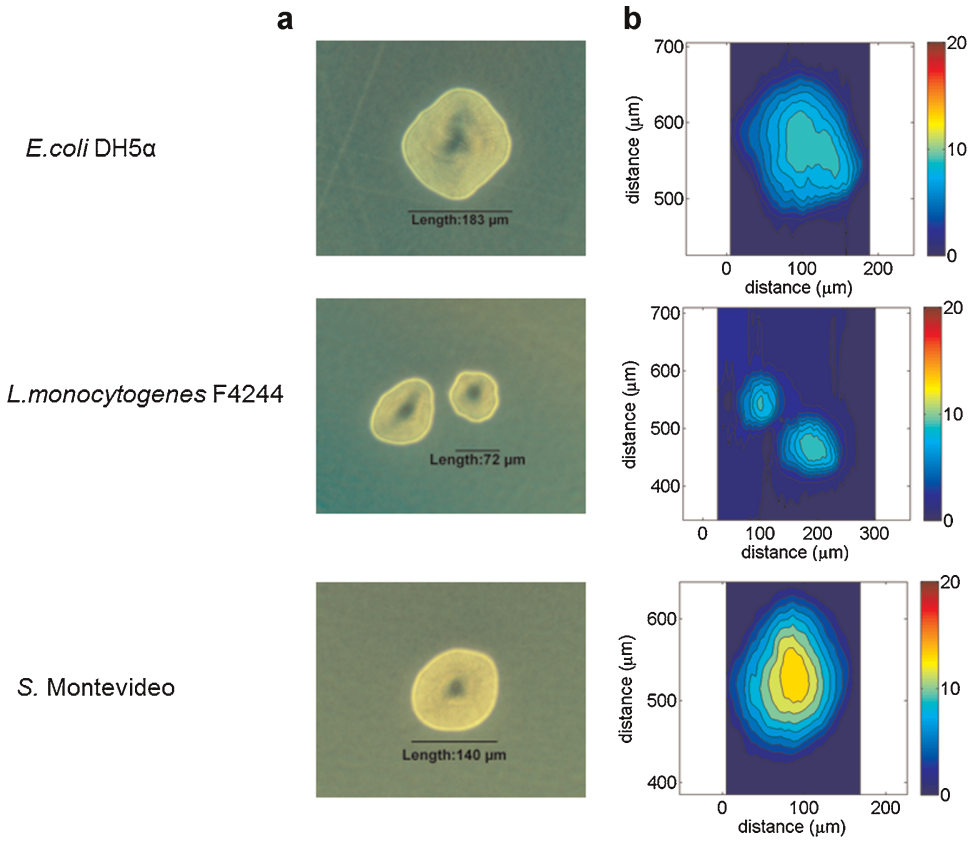

Figure 3. Microcolony morphology measurement for three different genera via (**a**) phase contrast microscope image which show the shape and diameter and (**b**) 2D contour plots of the 3D profile data from the CDM. [Color figure can be seen in the online version of this article, available at wileyonlinelibrary.com.]

Morphology of Microcolonies

Since the observations of Scattering Patterns Section were related to the amplitude and phase modulation of the microcolonies (Bae et al., 2007), it was critical to accurately measure the profile of the individual colony to both understand and correlate the colony shape to the forward scattering patterns. Figure 3 displays the morphology of the microcolonies for the three bacteria with PCM (Fig. 3a) and CDM (Fig. 3b). *E. coli* DH5α was measured to be 183 μm in diameter with the peak height of 9.3 μm, while the image for *L. monocytogenes* F4244 showed two closely located bacterial colonies with the smaller one measured to be at 72 μm with a 7 μm peak height. Finally, *S.*Montevideo demonstrated a 140 μm diameter with 14.5 μm in peak height. It is noteworthy to address that the aspect ratio (diameter/peak height) of the bacterial colony to reach a similar diameter is quite different for different genus under the same growth conditions.

Theoretical Modeling of Scattering From Microcolony

As reported in previous research, bacterial colony shape was assumed to be a Gaussian shape which enabled us to model the colony scattering response with two main parameters: The central thickness (H_0) and $1/e^2$ radius (w_b) Therefore, the experimentally measured profile data of each individual colony were fitted with Gaussian curves to estimate the two parameters. Subsequently, scalar diffraction theory was used to predict the forward scattering pattern generated by the colony. The coordinate system was defined in Figure 4a and the colony was treated as an optical phase $\Phi'(x_a,y_a)$ and amplitude $t(x_a,y_a)$ modulator with the fitted Gaussian cross-section as below (Bae et al., 2007, 2008, 2010):

$$E_2(x_i,y_i) \approx C_2 \iint_{\Sigma} t(x_a,y_a)\exp\left[-\frac{(x_a^2+y_a^2)}{w^2(z_1)}\right]\exp[ik\phi'(x_a,y_a)] \times \exp[-i2\pi(f_x x_a + f_y y_a)]\,dx_a\,dy_a \quad (1)$$

where (x_a,y_a) represented the aperture plane coordinates, (x_i,y_i) represents the image plane coordinates, w was the Gaussian beam waist of the incoming laser, z_1 was the distance from the source plane to the aperture plane, z_2 was the distance from the aperture plane to the detection plane, E_2 was the electrical field distribution on the detection

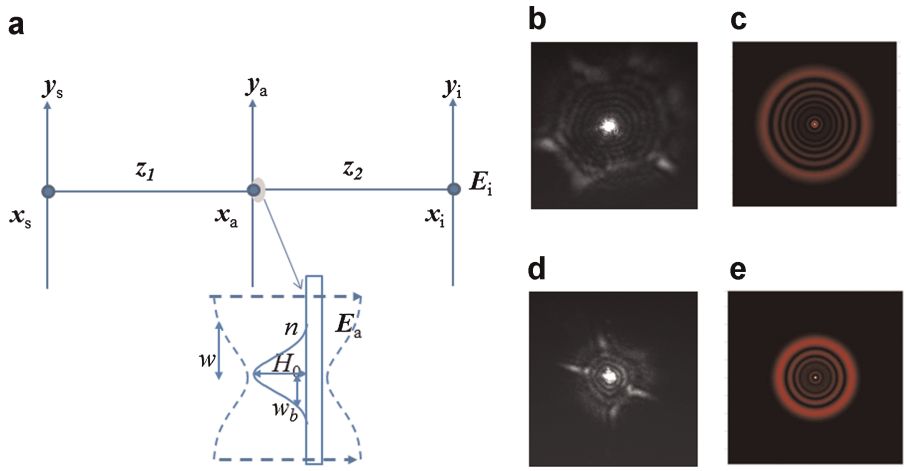

Figure 4. **a**: The schematic layout to define the coordinate systems and modeling parameters for predicting the scattering patterns from bacterial colonies. The incident laser starts at X_s, Y_s, and it is located with a distance of z_1 from the colony. X_a, Y_a, and E_a denote the aperture coordinates and the electrical field exiting the aperture plane, while X_i, Y_i, and E_i define the imaging coordinates and the electric field on the imaging plane at distance z_2 from the colony. (**b** and **d**) are experimental snapshots of the scattering patterns for *S.*Montevideo and *E. coli* DH5α; (**c** and **e**) display the predicted scattering patterns at $z = 30$ mm, $\lambda = 635$ nm, and $w = 45$ μm. The (H_0, w_b) were set to (14.46 and 42.8 μm) and (9.94 and 43.4 μm), respectively. [Color figure can be seen in the online version of this article, available at wileyonlinelibrary.com.]

plane, C_2 was a constant, and f_x and f_y was defined as $f_x = x_i/\lambda z_2$, $f_y = y_i/\lambda z_2$. To accurately model the phase modulation generated by a colony, we consolidated three optical phase contributions as:

$$\phi'(x_a, y_a) = \left[\left(\frac{x_a^2 + y_a^2}{2}\right)\left(\frac{1}{R(z_1)} + \frac{1}{z_2}\right) + (n_1 - 1)H_0\left(\exp\left(-\frac{x_a^2 + y_a^2}{w_b^2}\right)\right)\right] \quad (2)$$

where H_0 was the center thickness, w_b was the $1/e^2$ radius, n was the refractive index for colony, and $w(z)$ and $R(z)$ were the radius of the incoming Gaussian beam and its radius of curvature. First term represented the quadratic phase factor contributing from the incoming laser beam while the second term was from the Gaussian shaped bacterial colony. The amount of amplitude and phase modulation was estimated based on the profile information and a bacteria-stack-layer model with the assumption of homogeneous refractive index distribution within the colony. Figure 4b–e displays the experimental measurement and theoretical prediction of scattering patterns based on parameters estimated from the CDM data. Simulation was computed with $z = 30$ mm, $\lambda = 635$ nm and $w = 45$ μm while (H_0, w_b) were set to (14.46 and 42.8 μm) and (9.94 and 43.4 μm) for *S.*Montevideo and *E. coli* DH5α, respectively. Experimental measurements and simulation results closely resembled each other regarding the number of generated rings in the scattering patterns for both *S.*Montevideo and *E. coli* DH5α. Moreover, colonies with larger H_0 generate more rings and wider scattering. As we demonstrated in Scattering Patterns and Morphology of Microcolonies Sections, *L. monocytogenes* F4244 had an aspect ratio close to *S.*Montevideo. Therefore, when we used a Gaussian function to approximate the shape of these two microcolonies, they generated similar scattering patterns. However, microcolonies of *L. monocytogenes* F4244 showed circular and smooth edges which subsequently led to regular round-shaped scattering patterns opposite to the irregular ones from *S.*Montevideo and *E. coli* DH5α.

Morphology and Scattering Pattern Correlation

To quantitatively correlate colony shape with the forward scattering patterns, 1D cross-sections of the representative height profiles were compared. Figure 5a shows the aspect ratio comparison for three genera. The profile of *E. coli* DH5α (red-solid line) measured at approximately 200 μm in diameter with a 9.3 μm peak value, which provided an approximate 20:1 aspect ratio while S.Montevideo (blue-dotted line) and *L. monocytogenes* F4244 (green-dashed line) showed approximately 10:1 ratio. To further support our understanding, Figure 5b displays the aspect ratio distribution of ten microcolonies for each genus. The result clearly indicates a trend of 10:1 aspect ratio for *S.*Montevideo and *L. monocytogenes* F4244, while *E. coli* DH5α showed more of a "less raised" colony shape for this diameter regime. To understand the overall phenotypic characteristics of these three bacteria, we have plotted the three major characteristics in three dimensional space: Colony diameter (*X*-axis), number of rings (*Y*-axis), and incubation time (*Z*-axis). Figure 6 displays that each genus can be grouped separately to provide differentiations considering all the three phenotypic characteristics. *L. monocytogenes* F4244 was the slowest growing species, which separated itself from the

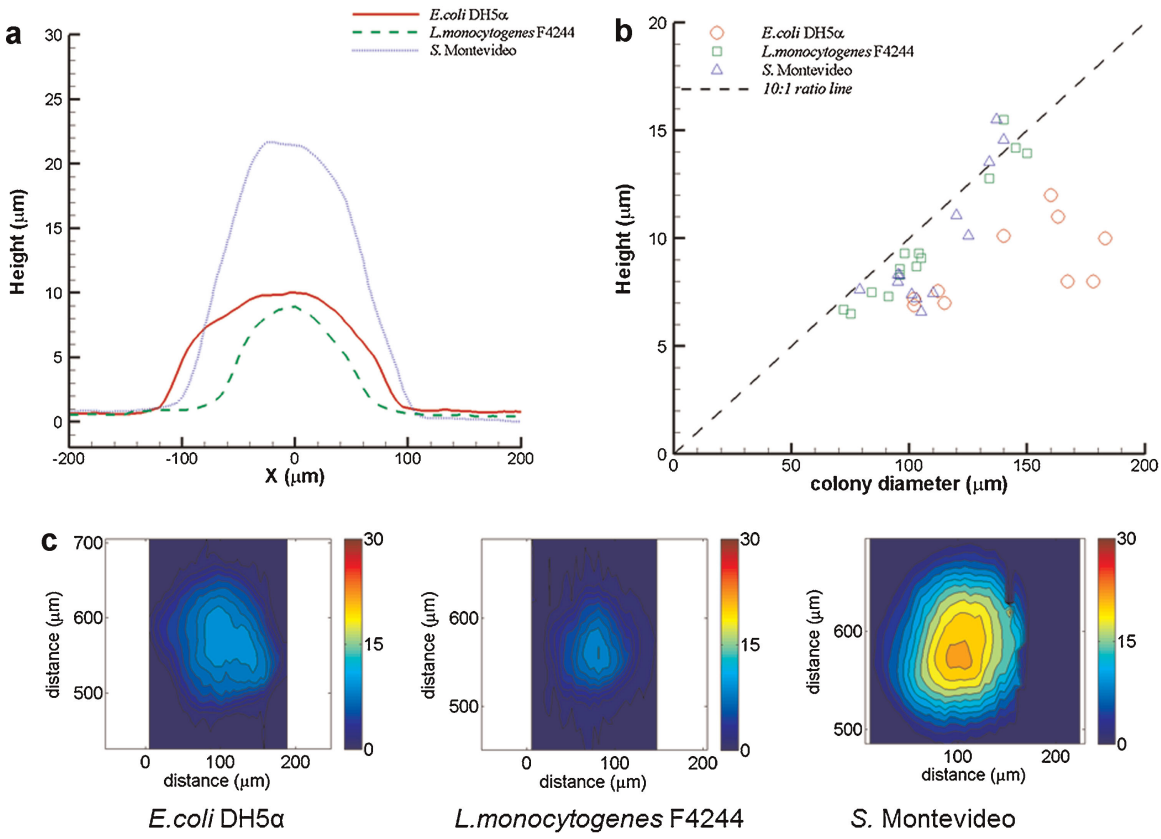

Figure 5. Profile comparison for three different bacteria: (**a**) 1D height profiles across the peak locations for *S.*Montevideo (blue-dotted line), *L. monocytogenes* F4244 (green-dashed line), and *E. coli* DH5α (red-solid line); (**b**) the aspect (diameter/height) ratio distributions with a 10:1 ratio line; (**c**) 2D contour plots of the 3D profile data used in (a) for plotting the cross section views. [Color figure can be seen in the online version of this article, available at wileyonlinelibrary.com.]

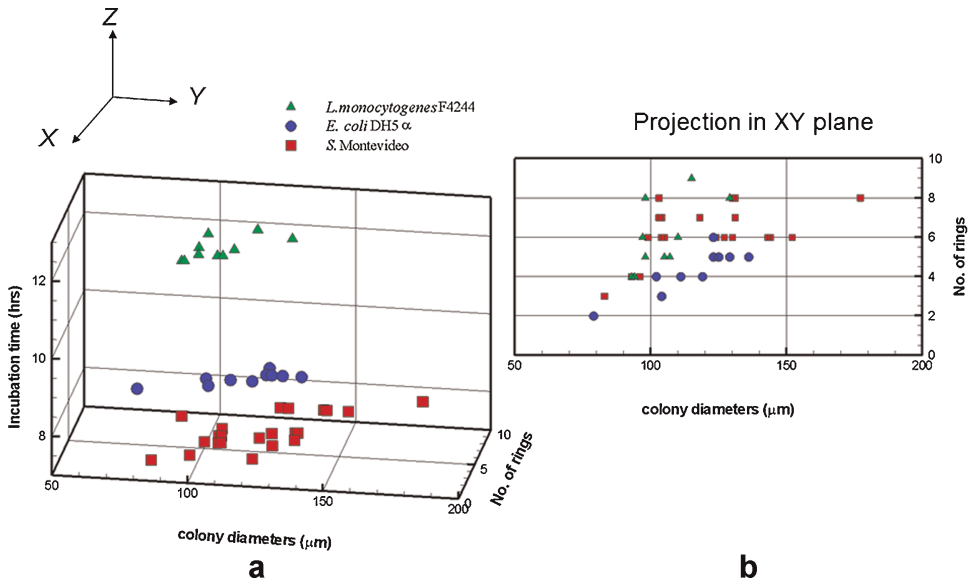

Figure 6. Representation of the phenotypic characteristics in three dimensional space for *E. coli* DH5α (9 h), *S.*Montevideo (7 h), and *L. monocytogenes* (12 h): (**a**) displays that these three bacteria can be differentiated based on colony diameter (*X*), number of rings (*Y*), and incubation time (*Z*); (**b**) is the projection plot on the *XY* plane to show the correlation between the colony diameter and the number of rings. Mean ring count of *E. coli* DH5α (4.3) is smaller than that of the *S.*Montevideo (6.1) and *L. monocytogenes* F4244 (5.9) which can be explained similarly as the aspect ratio of the colony (Fig. 5b). [Color figure can be seen in the online version of this article, available at wileyonlinelibrary.com.]

other two, while the number of rings generates sufficient separation between *S*.Montevideo and *E. coli* DH5α.

Discussion

The two major variations of the scattering patterns of Figure 2 are: (1) the number of rings was increasing as the colony diameter increased and (2) there were ring circularity differences among bacterial species. The first observation can be attributed to the phase modulation effect, ϕ, arising from the increasing optical path length difference (OPD). Since OPD is defined as:

$$\phi = knL \tag{3}$$

where k is the wavevector, n is the refractive index, and L is the physical path length, if we define the bacterial colony as a convex Gaussian profile, then the OPD can be modeled as:

$$\Delta\phi = (n-1)H_0 \exp\left(-\frac{r^2}{w_b^2}\right) + H_0. \tag{4}$$

This suggests that the OPD was proportional to the peak height which increased as the colony grows. The correlation of phase modulation and the observed diffraction rings was also commented in the Nematic liquid crystal research (Bloisi et al., 1988; Chen et al., 1998; Khoo et al., 1987; Ogusu et al., 1996). The authors pointed out the relationship of the phase modulation and the number of diffraction rings as:

$$N_{\text{ring}} \cong \frac{\Delta\Phi}{2\pi}. \tag{5}$$

If we apply Eq. (5) for *S*.Monetvideo (124 μm) assuming the 10:1 ratio, the expected number of rings are 6.8, where the actual ring count from the scattering pattern was 6 (assuming the bright central spot as a single ring count). Similarly, for *E. coli* DH5α (129 μm) the assumption of a 20:1 ratio resulted in 3.8 ring counts, while the experiment showed four rings.

The aspect ratio of *E. coli* DH5α was lower than the other two species, and this resulted in a fewer number of ring counts in the scattering patterns (Fig. 6b) at the same experimental conditions (mean ring count: *E. coli* DH5α (4.3), *S*.Montevideo (6.1), and *L. monocytogenes* F4244 (5.9)). In addition, the growth time to reach the designated diameter range also played an important role in differentiating bacteria species. This information was traditionally known to the microbiologist by experience, but we proposed to explore this parameter in a quantitative and holistic manner to be leveraged in microcolony identification. The scattering patterns for microcolonies showed less distinctive characteristics among different genera, compared to the previous results for macrocolonies (~1–1.3 mm), which showed diverse scattering patterns such as radial spokes, diffuse speckle, and secondary bright rings which were critical in the discrimination process. These features could be attributed to the complex microstructures and phase domains formed by extracellular polymeric substance excreted by bacteria and the role differentiation of bacteria within the colony during its formation and maturing process. However, in microcolonies, their morphology differences are more subtle, which requires a more thorough understanding of the growth and phenotypic characteristics and their correlations with the forward scattering patterns. Therefore, the proposed method demonstrates both promises and challenges for expanding this elastic scattering technique to microcolony differentiation. Further research will extend the current method to species level differentiation.

Conclusion

Microcolony differentiation via elastic light scattering was investigated for three different genera: *S* Montevideo, *L. monocytogenes* F4244, and *E. coli* DH5α. To accurately correlate the colony morphology to the scattering pattern, the CDM was used to measure the 3D height profiles of colonies at different diameters. The results indicate that growth characteristics of microcolonies are encoded in their shapes which can be extracted from the number of ring counts in the scattering patterns. Overall three morphological characteristics parameters (growth time, colony diameter, and ring count) were sufficient to differentiate the tested microcolonies in genus level.

This research was supported through a cooperative agreement with the Agricultural Research Service of the US Department of Agriculture project number 1935-42000-035 and the Center for Food Safety and Engineering at Purdue University.

References

Asano S, Iijima K, Suzuki K, Motoyama Y, Ogata T, Kitagawa Y. 2009. Rapid detection and identification of beer-spoilage lactic acid bacteria by microcolony method. J Biosci Bioeng 108(2):124–129.

Bae E, Aroonnual A, Bhunia AK, Robinson JP, Hirleman ED. 2009. System automation for a bacterial colony detection and identification instrument via forward scattering. Meas Sci Technol 20(1):015802.

Bae E, Bai N, Aroonnual A, Robinson JP, Bhunia AK, Hirleman ED. 2010. Modeling light propagation through bacterial colonies and its correlation with forward scattering patterns. J Biomed Opt 15(4):045001–0450011.

Bae E, Banada PP, Huff K, Bhunia AK, Robinson JP, Hirleman ED. 2007. Biophysical modeling of forward scattering from bacterial colonies using scalar diffraction theory. Appl Opt 46(17):3639–3648.

Bae E, Banada PP, Huff K, Bhunia AK, Robinson JP, Hirleman ED. 2008. Analysis of time-resolved scattering from macroscale bacterial colonies. J Biomed Opt 13(1):014010.

Banada PP, Huff K, Bae E, Rajwa B, Aroonnual A, Bayraktar B, Adil A, Robinson JP, Hirleman ED, Bhunia AK. 2009. Label-free detection of multiple bacterial pathogens using light-scattering sensor. Biosens Bioelectron 24(6):1685–1692.

Bloisi F, Vicari L, Simoni F, Cipparrone G, Umeton C. 1988. Self-phase modulcation in nematic liquid-crystal films – Detailed measurements and theoretical calucations. J Opt Soc Am B 5(12):2462–2466.

Bronk BV, Li ZZ, Czege J. 2001. Polarized light scattering as a rapid and sensitive assay for metal toxicity to bacteria. J Appl Toxicol 21(2):107–113.

Bronk BV, Vandemerwe WP, Stanley M. 1992. Invivo measure of average bacterial-cell size from a polarized-light scattering function. Cytometry 13(2):155–162.

Cash P. 2009. Proteomics in the study of the molecular taxonomy and epidemiology of bacterial pathogens. Electrophoresis 30(Suppl. 1): S133–S141.

Cash P, Hecker M. 2003. Proteomics of microorganisms. Advances in Biochemical Engineering/Biotechnology 83/2003: 93–115. DOI: 10.1007/3-540-36459-5_4

Chen SH, Fan JY, Wu JJ. 1998. Novel diffraction phenomenon with the first order Fredericksz transition in a nematic liquid crystal film. J Appl Phys 83(3):1337–1340.

Choo-Smith LP, Maquelin K, van Vreeswijk T, Bruining HA, Puppels GJ, Thi NAG, Kirschner C, Naumann D, Ami D, Villa AM, Orsini F, Doglia SM, Lamfarraj H, Sockalingum GD, Manfait M, Allouch P, Endtz HP. 2001. Investigating microbial (micro)colony heterogeneity by vibrational spectroscopy. Appl Environ Microbiol 67(4):1461–1469.

Cumming M, Kludt P, Matyas B, DeMaria A, Stiles T, Han L, Gilchrist M, Neves P, Fitzgibbons E, Condon S. 2009. Outbreak of Listeria monocytogenes infections associated with pasteurized milk from a local dairy-Massachusetts, 2007 (reprinted from MMWR, vol 57, pp. 1097–1100, 2008). JAMA 301(8):820–822.

Gehring AG, Albin DM, Irwin PL, Reed SA, Tu SI. 2006. Comparison of enzyme-linked immunomagnetic chemiluminescence with US Food and Drug Administration's Bacteriological Analytical Manual method for the detection of *Escherichia coli* O157: H7. J Microbiol Methods 67(3):527–533.

Goodwin JR, Hafner LM, Fredericks PM. 2006. Raman spectroscopic study of the heterogeneity of microcolonies of a pigmented bacterium. J Raman Spectrosc 37(9):932–936.

Heaton JC, Jones K. 2008. Microbial contamination of fruit and vegetables and the behaviour of enteropathogens in the phyllosphere: A review. J Appl Microbiol 104(3):613–626.

Jaradat ZW, Schutze GE, Bhunia AK. 2002. Genetic homogeneity among Listeria monocytogenes strains from infected patients and meat products from two geographic locations determined by phenotyping, ribotyping and PCR analysis of virulence genes. Int J Food Microbiol 76(1–2):1–10.

Jones A, Young D, Taylor J, Kell DB, Rowland JJ. 1998. Quantification of microbial productivity via multi-angle light scattering and supervised learning. Biotechnol Bioeng 59(2):131–143.

Keyence-Corporation. 2006. Surface Scanning Laser Confocal Displacement Meter LT-9001 Series. Keyence Corporation. Tokyo: Keyence Corporation.

Khoo IC, Hou JY, Liu TH, Yan PY, Michael RR, Finn GM. 1987. Transverse self-phase modulation and bstability in the transmission of a laser-beam through a nonlinear thin-film. J Opt Soc Am B 4(6):886–891.

King LA, Mailles A, Mariani-Kurkdjian P, Vernozy-Rozand C, Montet MP, Grimont F, Pihier N, Devalk H, Perret F, Bingen E, Espie E, Vaillant V. 2009. Community-wide outbreak of *Escherichia coli* O157: H7 associated with consumption of frozen beef burgers. Epidemiol Infect 137(6):889–896.

Kottmeier K, Weber J, Muller C, Bley T, Buchs J. 2009. Asymmetric division of hansenula polymorpha reflected by a drop of light scatter intensity measured in batch microtiter plate cultivations at phosphate limitation. Biotechnol Bioeng 104(3):554–561.

Motoyama Y, Yamaguchi N, Matsumoto M, Kagami N, Tani Y, Satake M, Nasu M. 2008. Rapid and sensitive detection of viable bacteria in contaminated platelet concentrates using a newly developed bioimaging system. Transfusion (Paris) 48(11):2364–2369.

Ogusu K, Kohtani Y, Shao H. 1996. Laser-induced diffraction rings from an absorbing solution. Opt Rev 3(4):232–234.

Samorski M, Muller-Newen G, Buchs J. 2005. Quasi-continuous combined scattered light and fluorescence measurements: A novel measurement technique for shaken microtiter plates. Biotechnol Bioeng 92(1):61–68.

Shetty A, McLauchlin J, Grant K, O'Brien D, Howard T, Davies EM. 2009. Outbreak of Listeria monocytogenes in an oncology unit associated with sandwiches consumed in hospital. J Hosp Infect 72(4):332–336.

Siegman AE. 1986. Lasers. Sausalito: University Science Books.

Stecchini ML, Del Torre M, Donda S, Maltini E. 2000. Growth of *Bacillus cereus* on solid media as affected by agar, sodium chloride, and potassium sorbate. J Food Prot 63(7):926–929.

Swaminathan B, Gerner-Smidt P. 2007. The epidemiology of human listeriosis. Microbes Infect 9:1236–1243.

Tetz VV, Rybalchenko OV, Savkova GA. 1993. Morphophysicological characteristics of *Escherichia coli* and Shigella-Flexneri 2A carrying the HTPR15 Gene. J Basic Microbiol 33(2):131–139.

Van Duynhoven Y, Isken LD, Borgen K, Besselse M, Soethoudt K, Haitsma O, Mulder B, Notermans DW, De Jonge R, Kock P, Van Pelt W, Stenvers O, Van Steenbergen J. 2009. A prolonged outbreak of *Salmonella typhimurium* infection related to an uncommon vehicle: Hard cheese made from raw milk. Epidemiol Infect 137(11):1548–1557.

Wang XD, Yamaguchi N, Someya T, Nasu M. 2007. Rapid and automated enumeration of viable bacteria in compost using a micro-colony auto counting system. J Microbiol Methods 71(1):1–6.

Wyatt PJ. 1969. Identification of bacteria by differential light scattering. Nature 221(5187):1257.